Optic Disc Segmentation in Fundus Images Using Anatomical Atlases with Nonrigid Registration

Ambika Sharma[1], Dr. Monika Aggarwal[1], Dr. Sumantra Dutta Roy[1], Dr. Vivek Gupta[2], Dr. Praveen Vashist[2], and Dr. Talvir Sidhu[2]

[1] Indian Institute of Technology Delhi (IITD)
[2] All Indian Institute of Medical Sciences (AIIMS) Delhi
New Delhi

Abstract. According to a WHO report, approximately 253 million people live with vision impairment, 36 million of which are blind and 217 million have moderate to severe vision impairment. In a recent estimate, the major causes of blindness are Cataract, Uncorrected refractive index, and Glaucoma. Thus in medical diagnosis, the retinal image analysis is a very vital task for the early detection of eye diseases such as Glaucoma, diabetic retinopathy (DR), Age-macular Degeneration (AMD) etc. Most of these eye diseases, if not diagnosed at an early stage might lead to permanent loss of vision.

A critical element in the computer-aided diagnosis of Digital Fundus images is the automatic detection of the optic disc region. Especially for the Glaucoma case, where cup to disc diameter ratio (CDR) is the most important indicator for detection. In this paper, we present a nonrigid registration based robust optic disc segmentation method using image retrieval based optic disc model maps that detect optic disc boundaries and surpasses the state-of-the-art performances. The proposed method consists of three main stages: 1) a content-based image retrieval from the model maps of OD using Bhattacharyya shape similarity measure, 2) constructing the test image specific anatomical model using the SIFT-flow technique for deformable registration of training masks to the test image OD mask, and 3) extracting the optic disc boundaries using a thresholding approach and smoothen the image by applying morphological operations along with the final ellipse fitting. The proposed work has used three datasets RIM, DRIONS and DRISHTI with 835 images in total. Our average accuracy values for 685 test images is 95.8%. The other performance parameter values are Specificity is 95.54% , Sensitivity is 96.13%, Overlap is 86.46% and Dice metric is 0.924 respectively, which clearly demonstrates the robustness of our optic disc segmentation approach.

Keywords: Computer Vision, Image registration, Retinal Image, Optic Disc,computer-aided detection(CAD), Morphology, Optic disc(OD).

1 Introduction

According to current eye disease statistics more than 42 million people are currently blind in the world, 80 percent of which could have been prevented or cured by early detection [1],[16]. India is the second most populous country in the world and shares 17.5 percent of the world's population. Thus, in case of any health problem lead to a rapid increase in global morbidity rate. Currently, India has more than 15 million blind people, which is expected to increase to 16 million by 2020 [3][16]. Some of the most prevailing eye diseases are Cataract, Glaucoma, Diabetic retinopathy and Age-related macular degeneration. Glaucoma is the second leading cause of blindness in the world. It is also called silent-thief as the progression of disease is gradual and one might not able to diagnose it at early stage. In developing countries most of the population lives in remote and rural areas, therefore, it is not possible to reach out with due to a limited number of trained opticians and resources. As mentioned in[17], that eight minutes per eye is needed for complete segmentation of optic disc and cup. Thus, there is great need to have a cost-effective automatic computer-based diagnostic systems to enable even the people in remote and rural areas to get a medical diagnosis in time. Also, this CAD system will provide a preliminary evaluation of the patient's eye. Using Internet of things (IOT) based techniques we can further develop a system where the patients periodically test their eye while sitting at home using a handheld device and diagnostic system will evaluate the patient parameters which can further be uploaded into the virtual cloud and finally can be retrieved by the professionals at any time. This not only saves the doctor's time and effort but makes the procedure plat-form independent i.e. it will be able to work under different environment conditions where no instructions from a medical practitioner are necessary and able to interpret the results sensibly.

For the screening of most of the eye diseases, the detection and segmentation of optic disc is an important step. For e.g. in Glaucoma professionals look for the cup to disc diameter ratio (CDR) as the key parameter for the diagnosis. The optic nerve examination includes the analysis of a fundus (retinal) image, which is the photograph of the inner surface of the eye opposite to lens and includes different anatomical structures (features) like retina, optic disc, macula, fovea and blood vessels. In a healthy fundus image with good contrast and resolution, segmentation of the optic disc is a tractable problem, but the situation becomes difficult when the pathological condition occurs. In a diseased fundus image, the contrast is no longer uniform and segmenting the region of interest becomes a challenging task.

A number of methods have been proposed for the optic disc segmentation. Some of the traditional image processing techniques used template matching approach along with highly saturated intensity in red channel for disc segmentation [3],[4],[5].Abdel-Ghafar et al.[20] proposed a simple segmentation technique based on the edge detector and the circular Hough transform (CHT). The method uses the green channel for processing as it has the highest contrast and

morphological operations are used to remove the blood vessels. After applying the Sobel operator to the green channel, the image is thresholded and resulting points are given as input to the circular Hough transform. The algorithm claims that the largest circle was consistently found to be an optic disc with its center as the approximated OD center. A watershed-based OD segmentation approach is proposed by Welfer et al. [21]. Other methods have used circular Hough Transform [9] and region growing techniques [11] with a prior knowledge of seed point in the region of interest. Active shape model [11] based techniques such as changes method for active contours [11] have been very popular in the medical imaging, but they fail to extract the exact boundary of optic disc in case of low gradient between optic disc and background and when the PPA region is present around OD which has the same color characteristics as that of optic disc. Also, AC based methods often fail to control the contour formation process as they either terminate far outside or inside the OD boundary. Additional challenges include segmenting the low quality and blurred images, making allowances for anatomical variations in resolution, contrast and optic disc inhomogeneities. Fig1 shows some examples of such variations like poor contrast and PPA.

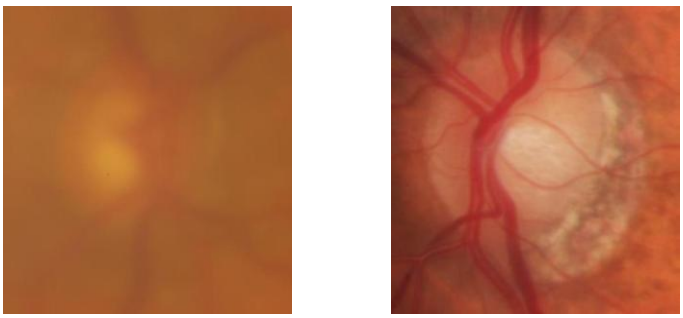

Fig. 1. Example of blurred and pathological Optic disc

In this paper for optic disc segmentation, we presented a robust automated optic disc segmentation system for retinal images. Our method mainly consists of three main stages as shown in the proposed architecture in Fig. 2. In the first subsection of the method we have build a anatomical model maps for optic disc with pre-segmented masks being marked by experts. The top 5 similar masks have been selected based on similarity coefficient between test image and model masks. The highly ranked masks retrieved by this method are usually a good fit for the test fundus image. In the second subsection, for the chosen masks the method first calculates the corresponding pixels between the test image and each of the model images which provides the transformation mapping for each of the pixel. Finally, it aligns the model masks using the transformation mapping. In the last subsection a thresholding has been applied to the combined segmented

masks obtained by summing the outputs from each of the model map transformation. In order to smooth the optic disc boundary morphological closing has been used along with the ellipse fitting as optic disc is slightly vertically oval as per the literature. A detailed assessment of the approach compared to other state-of-the-art methods have been discussed in the later sections. In Fig. 2 the test image has been compared with the Atlas images using projection profile knowledge and the best five masks have been selected based on Bhattacharyya coefficient. Finally, SIFT features comparison is done between target image and given image in order to warp the model mask into the desired test optic disc mask. In the last step, the obtained probabilistic mask has been thresholded to get the segmented binary image. The proposed approach has huge advantage for the OD segmentation as it uses both prior knowledge of optic disc (unlike other model based approaches e.g. active contour) and require less amount of images in the atlas dataset(unlike machine learning models). Moreover as medical images are subjective in nature, this approach has helped us in handling this subjectivity.

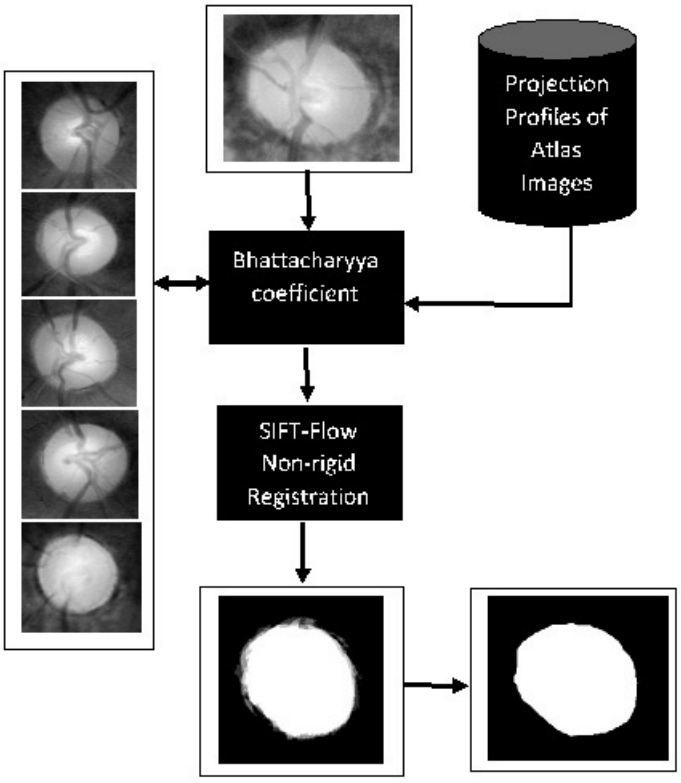

Fig. 2. Proposed Architecture for Optic Disc Segmentation

2 Proposed Method

2.1 CBIR Model from the Fundus Atlas for Inter-Image Matching

The Optic disc is a bright circular region in a fundus image. According to literature [5], disc is the brightest portion in the red channel of the retinal image. For the extraction of disc boundary, we have used a pre-processing step of cropping the Region of Interest from the complete retinal image and to do so we have used the work of [6] on optic disc detection i.e. finding a point inside the optic disc boundary, in order to have a initial seed point for cropping the region for the optic disc. The algorithm uses the vessel convergence property at the optic disc along with the disc characteristics (shape, size, and colour) to find a point inside the disc boundaries. The RIM dataset contains the cropped region having ROI as OD portion, but for DRISHTI and DRIONS the above mentioned pre-processing step has been implemented.

The segmentation task in medical imaging poses a number of challenges such as light artifacts while capturing images, dust particles, multiplicative noise, motion during imaging, low contrast, sampling artifacts caused by acquisition equipment and finally anatomical variations due to pathological conditions.Therefore, using classical segmentation methods like gradient, and thresholding based, which do not have a prior knowledge of the object to be segmented, usually produce unsatisfactory results on medical images. Thus in order to solve the above problem, we proposed a retinal image atlas dataset into the system which gives variation in sizes, shapes, position with respect to the optic disc.The atlas images have been created by selecting the best optic disc images i.e. those images which contain no pathology like peripheral atrophy (PPA) or disc haemorrhage around the optic disc boundary. All these atlas images have been manually labelled, in consultation with retinal specialists. The atlas construction has been done in such a way that it covers all varieties of optic disc in terms of shape, size and color.

For the test image, we first identify a subset of images (i.e. five in our case) from the model maps that are most similar to the test fundus ROI image, using a content-based image retrieval (CBIR) inspired approach, and use this subset of training images including their corresponding OD masks to develop a test image specific OD model. The content based image retrieval has been done by calculating the intensity projection profiles along vertical and horizontal directions. For the atlas images the horizontal and vertical projection profiles are pre-computed in order to speed up the CBIR search process. For the similarity measurement between two distributions of test image and the atlas images Bhattacharyya coefficient has been used, which is as follows:

$$BC(I_1, I_2) = \alpha \sum_{x=1}^{n} \sqrt{p_1(x)p_2(x)} + (1-\alpha) \sum_{y=1}^{m} \sqrt{q_1(y)q_2(y)} \qquad (1)$$

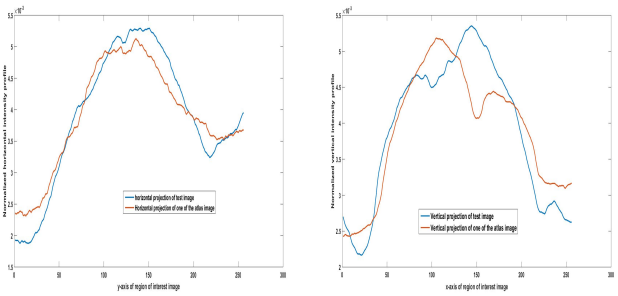

Fig. 3. Plot shows the horizontal(left) and vertical(right) projection profiles of test and one of the atlas image

where $p_1(x)$ and $p_2(x)$ are the horizontal projections, $q_1(y)$ and $q_2(y)$ are the vertical projections of images I_1 and I_2 images respectively, x and y are the histogram bins of the projection profiles and n and m are the number of bins of the projection profiles and profile histograms and $\alpha = \frac{n}{n+m}$. The value of α varies for 0 to 1, but for the experimental work we have $n = m$ and thus results into $\alpha = 0.5$.

Fig. 3 shows the horizontal and vertical profile histograms of an example image. Left image shows the horizontal projection profile between the test image and one of the best matching atlas image and right image shows the vertical projection profile respectively. The other distance metrics used in literature[31] for similarity measurement are Euclidean, Manhatten etc but the chosen coefficient give the best possible performance under given conditions. We select a set of best fit training atlases from the anatomical database of segmented optic disc images to learn a test specific OD model. The registration performance for our method is significantly improved when a personalized OD model is designed by comparing the test ROI with the pre-segmented optic disc images in the database using a fast similarity measure based on Bhattacharyya coefficient.

In our proposed work, the similarity index has been calculated for both red and green channels, as red channel represents the saturated optic disc region for healthy images and thus works for most of the cases, but for abnormal conditions, the green channel performs better. Thus, the best channel has been selected based on the performance parameter value being calculated.

2.2 SIFT-Flow Deformable Warping of OD Atlas

Image registration scheme calculates a transformation mapping from the source image to target image by matching corresponding pixels of the images. The local image feature descriptors such as Scale Invariant Feature Transform(SIFT)[28], Histogram of Gradient(HOG)[29], shape and curvature descriptors can be used to match the correspondence. In this work, we used the SIFT descriptor which is among the best performing local image feature descriptors.

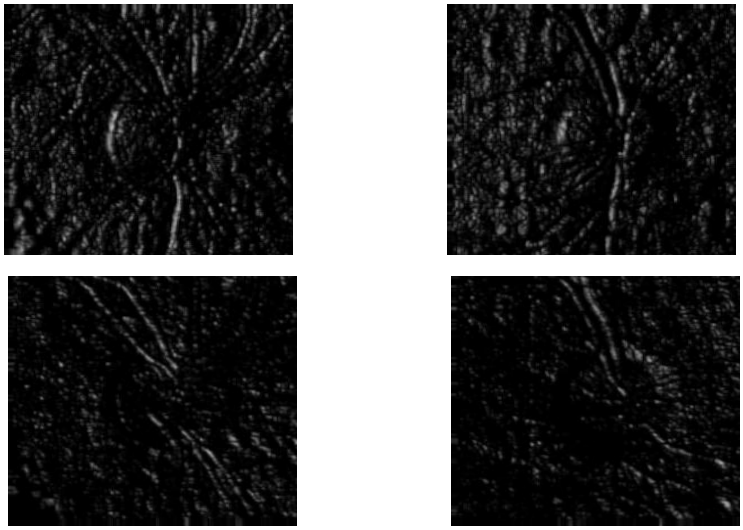

Fig. 4. SIFT descriptors for test image(1st column) and atlas image(2nd column) respectively.

In computer vision image alignment remains a difficult task and the goal becomes even more difficult in the object recognition scenario, where the goal is to align different instances of the same object category. Similar to well known computer vision image alignment technique of optical flow where an image is aligned to its temporally adjacent frame, we used SIFT flow [30], a method to align an image to its nearest neighbors in a database containing a variety of objects. The SIFT features allow robust matching across different scene/object appearances, whereas the discontinuity preserving spatial model allows matching of objects located at different parts of the scene. Experiments show that the proposed approach robustly aligns complex scene pairs containing significant spatial differences. Our work is focused on inter-image similarity with deformable warping for creating a test image specific OD atlas. We found that the SIFT-flow algorithm worked well for this task. The SIFT features of the ROI are calculated as follows. First, image gradient magnitude and orientation are computed at each pixel. The gradients are weighted by a Gaussian pyramid in a $K \times K$ region. Then the regions are subdivided into $k \times k$ quadrant. The histogram of gradient orientations is calculated for 8 bins for each of the quadrant. Finally the orientation histograms are concatenated to construct the SIFT descriptor for the center pixel in all $K \times K$ regions. In definition of SIFT descriptors K, and k are chosen to be 16 and 4 respectively [30], thus for each pixel we have a 128 dimensional feature vector. We have shown in Fig. 4 two such SIFT images (also called per-pixel sift descriptor) corresponding to test image (on left) and an atlas image (on right side).
Once the SIFT descriptors haven been calculated for the image, the registration

algorithm computes the correspondence between the test image and the atlas image by matching the SIFT descriptors. The SIFT flow algorithm consists of matching densely sampled, pixel-wise SIFT features between two images, while preserving spatial discontinuities[30].
The algorithm applies the transformation mapping by shifting each pixel in the atlas OD masks according to the calculated shift distances being given by the flow vectors. The registration stage is repeated for each of the top chosen masks (5 in our case). The obtained OD mask for the test image is calculated by adding all the transformed masks from each of the atlas OD regions and each pixel in the image represents the confidence level of the specific pixel belonging to the optic disc region.

2.3 Thresholding with mask smoothing

The obtained probabilistic masks can be smoothed further in order to enhance the robustness of the method. A smoothing filter is then applied on the decision values to achieve a smoothed decision value. In our implementation, mean filter and Gaussian filter are tested and the mean filter is found to be a better choice for the case. The smoothed decision values are then used further to calculate the binary decisions for all pixels using a threshold. A threshold value of 0.7 has been calculated empirically for all set of test images.
In our experiments, we have assigned a +1 and 0 to the disc(object) and non-disc(background) samples. An image closing morphological operations has been applied for disc shaped structuring element in order to remove the spikes present at disc boundary. At last, for smooth and continuous boundary ellipse fitting is done to the segmented optic disc region. Mostly medical experts label the optic disc as smooth curve, and to get that smoothness ellipse has been fitted. In fact this fitting has not changed the performance to a large extend (a little improvement by 0.3% in accuracy has been observed after ellipse fitting).

3 Experimental Results

3.1 Digital Retinal Image Datasets

The proposed method is evaluated using three different retinal databases, these are DRISHTI-GS1 dataset of 101 images [15],[18] provided by Medical Image Processing (MIP) group, IIIT Hyderabad, DRIONS dataset of 110 images and finally RIM(RIM-1 and RIM-2) dataset of 624 images. In DRISHTI-GS1 dataset all images were taken with the eyes dilated, centered on OD with a Field-of-View of 30-degrees and of dimension 2896 x 1944 pixels and PNG uncompressed image format. The optic disc has been marked by experts for all 101 images.
The DRIONS database consists of 110 colour digital retinal images.The images were acquired with a colour analogical fundus camera, approximately centred on the ONH and they were stored in slide format. In order to have the images in digital format, they were digitised using a HP-PhotoSmart-S20 high-resolution

scanner, RGB format, resolution 600x400 and 8 bits/pixel. The optic disc annotations have been done by two medical experts using a software tool.
Finally the RIM-1 database contains 169 optic nerve head images and each image has 5 manual segmentation from ophthalmic experts.The RIM-2 database consists of 455 images with disc annotated by the experts.

Fig. 5 shows a subset of test images with the expert labeling in black color along with segmented OD boundary in green color respectively. The proposed method gives pretty good performance for DRISHTI and DRIONS datasets. Also for the RIM database which contains most of the PPA, blurred and poor intensity images the method gives satisfactory performance as shown in Fig. 5 last row images. The key advantage of the proposed method is that it works for inter database images i.e. in RIM database most of the portion of ROI is covered by the OD region whereas in DRIONS and DRISHTI the OD takes a small portion of the complete ROI. So, in spite of the OD size variability for a fixed image dimension the proposed method is able to extract very good estimation of the true OD boundary.
For the designing of atlas retinal images we have selected a subset of images from each of the datasets. The anatomical atlas consists of 85 RIM images from 624 images, 35 DRISHTI-GS images from a set of 101 images and 31 images from the 110 DRIONS images respectively. Thus in total 150 retinal images have been selected for the atlas model and 724 images is used for testing purpose.

3.2 Evaluation Metrics

In the literature several algorithms have proposed different evaluation metrics for the segmentation purpose. The validation metrics True positive(TP), True negative(TN), False positive(FP), and False negative(FN) have been used for verifying the quality of segmented image. Here TP, FP, TN, FN represents the pixels correctly classified as foreground,falsely classified as foreground, correctly detected as background, and falsely detected as background respectively. All the metrics used have been calculated pixel-wise. In our work of comparing the performance of proposed method with the state-of-the-art we have used these above metrics to find the Accuracy, Specificity, Sensitivity, Region Overlap and Dice metric. Their mathematical expressions have been given below:

$$(ACC)Accuracy(A,B) = \frac{(TP+TN)}{(P+N)} * 100 \tag{2}$$

$$(SPE)Specificity(A,B) = \frac{TN}{(TN+FP)} * 100 \tag{3}$$

$$(SEN)Sensitivity(A,B) = \frac{TP}{(TP+FN)} * 100 \tag{4}$$

$$(DM)DiceMetric(A,B) = \frac{2*TP}{FP+2*TP+FN} \tag{5}$$

$$(OL)RegionOverlap = \frac{TP}{(TP+FN+FP)} * 100 \tag{6}$$

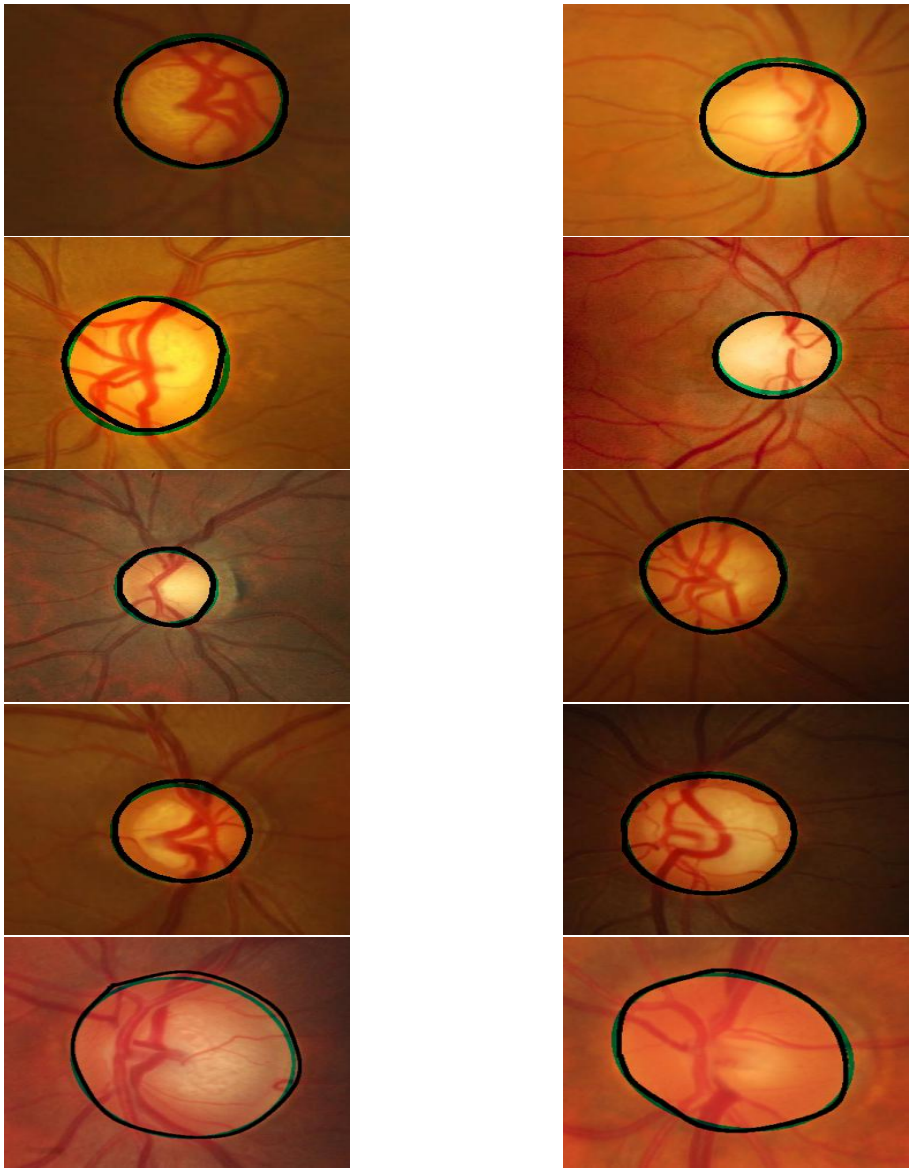

Fig. 5. Optic disc segmentation results. Here green and black colour represents the proposed and expert boundary respectively

For Bhattacharyya coefficient calculation, the value of $\alpha = 0.5$ has been considered as the image has been interpolated to square image.

Table 1. Proposed algorithm performance parameters for different databases

	ACC	SPE	SEN	OL	DM
Datasets					
RIM	94.89	94.49	95.95	84.89	0.92
DRISHTI	99.15	99.43	97.38	93.44	0.96
DRIONS	99.30	99.50	96.55	90.64	0.95
AVG Perf.	97.88	97.81	96.56	89.66	0.95

Table 1 shows the performance parameter values for all the datasets along with the average performance of the proposed algorithm. We can see that the proposed method works well for DRISHTI and DRIONS datasets and also for the RIM dataset which contains most of the PPA images along with the blurred and intensity artifacts one's. The performance of proposed method for DRIONS, RIM and DRISHTI-GS datasets can be compared with state-of-the-art methods as shown in Table 2,3, and 4 respectively.

Table 2. Comparison of methods for optic disc segmentation for DRIONS Database. The symbol "-" represents no result has been reported for the case

	ACC	SPE	SEN	OL	DM
Methods					
Walter et al.[25]	-	-	-	-	0.612
Morales et al.[26]	99.34	-	-	-	0.9084
CHT and Graph cut[27]	95.0	99.0	85.0	85.0	0.91
DRIU[22]	94.89	94.49	95.95	84.89	0.92
Zilly et al.[23]	99.15	99.43	97.38	93.44	0.96
Proposed Method	99.3	99.5	96.45	90.64	0.95

Table 3. Comparison of methods for optic disc segmentation for RIM Database. The symbol "-" represents no result has been reported for the case

	ACC	SPE	SEN	OL	DM
Methods					
Lu's[12]	91.0	-	-	-	-
DRIU[22]	-	-	-	88.0	0.97
Zilly et al.[23]	-	-	-	89.0	0.94
Proposed Method	96.21	97.9	92.33	88.0	0.94

Table 4. Comparison of methods for optic disc segmentation for DRISHTI-GS Database. The symbol "-" represents no result has been reported for the case

	ACC	SPE	SEN	OL	DM
Methods					
DRIU[22]	-	-	-	88.0	0.97
Zilly et al.[23]	-	-	-	-	-
A Sev.[24]	-	-	-	89.0	0.94
Joshi et al.[15]	-	-	-	-	0.96
Proposed Method	99.15	99.42	97.28	93.44	0.96

4 Conclusion

We have presented a robust optic disc boundary detection method that is based on a test image specific atlas using the projection profile similarity selection and SIFT-flow nonrigid registration with refinement using filter smoothing and thresholding. We evaluated the algorithm on 712 test images with normal and pathological optic disc regions using three different databases. The experimental results showed an accuracy of 95.8% compared to expert segmentation gold standard. The other performance parameter values are Specificity is 95.54% , Sensitivity is 96.13%, Overlap is 86.46% and Dice metric is 0.924 respectively.

References

1. World Health Organization, Media centre: Visual impairment and blindness, Retrived from http://www.who.int/mediacentre/factsheets/fs282/en/, pp. 25, 2014.
2. A. Hoover and M. Goldbaum, Locating the optic nerve in a retinal image using the fuzzy convergence of the blood vessels, Med. Imaging, IEEE Trans., vol. 22, no. 8, pp. 951958, 2003.
3. J. Lowell et al., Optic nerve head segmentation, IEEE Trans Med Imaging, vol. 23, no. 2, pp. 256264, 2004.
4. V. Kumar and N. Sinha, Automatic Optic Disc segmentation using maximum intensity variation, IEEE 2013 Tencon - Spring, TENCON Spring 2013 - Conf. Proc., pp. 2933, 2013.
5. J. Lowell et al., Optic nerve head segmentation, IEEE Trans Med Imaging, vol. 23, no. 2, pp. 256264, 2004.
6. A. Sharma, M. Agrawal and B. Lall, "Optic Disc Detection Using Vessel Characteristics and Disc Features," 2017 Twenty-third National Conference on Communications (NCC), Chennai, 2017, pp. 1-6.doi: 10.1109/NCC.2017.8077135.
7. F. Yin et al., Automated segmentation of optic disc and optic cup in fundus images for glaucoma diagnosis, Proc. - IEEE Symp. Comput. Med. Syst., 2012.
8. D. K. Wong et al., Level-set based automatic cup-to-disc ratio determination using retinal fundus images in ARGALI., Conf. Proc. IEEE Eng. Med. Biol. Soc., vol. 2008, no. 2, pp. 22662269, 2008.
9. A. Gopalakrishnan, A. Almazroa, K. Raahemifar, V. Lakshminarayanan, and A. Preprocessing, Optic Disc Segmentation using Circular Hough Transform and Curve Fitting, vol. 1, 2015.

10. S. Lu, Accurate and Efficient Optic Disk Detection and Segmentation by a Circular Transformation, IEEE Trans. Med. Imaging, vol. 30, no. 12, pp. 21262133, 2011.
11. M. Airouche, L. Bentabet, and M. Zelmat, Image Segmentation Using Active Contour Model and Level Set Method Applied to Detect Oil Spills, Proc. World Congr. Eng., vol. 1, no. 1, pp. 13, 2009.
12. S. Lu, Accurate and Efficient Optic Disk Detection and Segmentation by a Circular Transformation, IEEE Trans. Med. Imaging, vol. 30, no. 12, pp. 21262133, 2011.
13. Sevastopolsky A., Optic disc and cup segmentation methods for glaucoma detection with modification of U-Net convolutional neural network, Pattern Recognition and Image Analysis 27 (2017), no. 3, 618624
14. O. Ronneberger, P. Fischer, and T. Brox, U-net: Convolutional networks for biomedical image segmentation, in International Conference on Medical Image Computing and ComputerAssisted Intervention, pp. 234241, Springer, 2015.
15. J. Sivaswamy, S. Krishnadas, G. D. Joshi, M. Jain, and A. U. S. Tabish, Drishtigs: Retinal image dataset for optic nerve head (onh) segmentation, in Biomedical Imaging (ISBI), 2014 IEEE 11th International Symposium on, pp. 5356, IEEE, 2014
16. Vision 2020: The Right to Sight, IABP, Global-facts Retrived from http://www.iapb.org/vision-2020/what-is-avoidable-blindness/glaucoma.
17. G. Lim, Y. Cheng, W. Hsu, and M. L. Lee, Integrated optic disc and cup segmentation with deep learning, in Tools with Artificial Intelligence (ICTAI), 2015 IEEE 27th International Conference on, pp. 162169, IEEE, 2015.
18. J. Sivaswamy et al., A comprehensive retinal image dataset for the assessment of glaucoma from the optic nerve head analysis, JSM Biomedical Imaging Data Papers, vol. 2, no. 1, 2015.
19. Olaf Ronneberger, Philipp Fischer, Thomas Brox., "U-Net: Convolutional Networks for Biomedical Image Segmentation," Computer Vision and Pattern Recognition (cs.CV), MICCAI 2015, arXiv:1505.04597 [cs.CV]
20. R. A. Abdel-Ghafar and T. Morris (2007) Progress towards automated detection and characterization of the optic disc in glaucoma and diabetic retinopathy, Medical Informatics and the Internet in Medicine, 32:1, 19-25, DOI: 10.1080/14639230601095865
21. D. Welfer, J. Scharcanski, C. M. Kitamura, M. M. Dal Pizzol, and D. R. Marinho, Segmentation of the optic disk in color eye fundus images using an adaptive morphological approach, Comput. Biol. Med., vol. 40, no. 2, pp. 124137, 2010.
22. K.-K. Maninis, J. Pont-Tuset, P. Arbelaez, and L. Van Gool, Deep retinal image understanding, in International Conference on Medical Image Computing and Computer-Assisted Intervention,pp. 140148, Springer, 2016.
23. J. Zilly, J. M. Buhmann, and D. Mahapatra, Glaucoma detection using entropy sampling and ensemble learning for automatic optic cup and disc segmentation, Computerized Medical Imaging and Graphics, vol. 55, pp. 2841, 2017
24. Sevastopolsky, Artem, "Optic Disc and Cup Segmentation Methods for Glaucoma Detection with Modification of U-Net Convolutional Neural Network", Pattern Recognition and Image Analysis, vol. 27, DO - 10.1134/S1054661817030269
25. Walter et al. (2002) Walter T, Klein J-C, Massin P, Erginay A. A contribution of image processing to the diagnosis of diabetic retinopathy-detection of exudates in color fundus images of the human retina. IEEE Transactions on Medical Imaging. 2002;21:12361243. doi: 10.1109/TMI.2002.806290.
26. Morales et al. (2013) Morales S, Naranjo V, Angulo J, Alcaiz M. Automatic detection of optic disc based on PCA and mathematical morphology, IEEE Transactions on Medical Imaging. 2013;32:786796. doi: 10.1109/TMI.2013.2238244.

27. Abdullah, Muhammad, Muhammad Moazam Fraz, and Sarah A. Barman. Localization and Segmentation of Optic Disc in Retinal Images Using Circular Hough Transform and Grow-Cut Algorithm. Ed. Henkjan Huisman. PeerJ 4 (2016): e2003. PMC. Web. 10 Aug. 2018.
28. D. Lowe, "Distinctive image features from scale-invariant keypoints," Int. J. Comput. Vis., vol. 60, no. 2, pp. 91-110, 2004.
29. A. Satpathy, X. Jiang and H. Eng, "Extended Histogram of Gradients feature for human detection," 2010 IEEE International Conference on Image Processing, Hong Kong, 2010, pp. 3473-3476.doi: 10.1109/ICIP.2010.5650070
30. C. Liu, J. Yuen and A. Torralba, "SIFT Flow: Dense Correspondence across Scenes and Its Applications," in IEEE Transactions on Pattern Analysis and Machine Intelligence, vol. 33, no. 5, pp. 978-994, May 2011. doi: 10.1109/TPAMI.2010.147
31. J.K Chung, P.L Kannappan, C.T Ng, P.K Sahoo,"Measures of distance between probability distributions", in Journal of Mathematical Analysis and Applications, Volume 138, Issue 1, Pages 280-292,1989